3D $^{15}N-^{13}C-^{13}C$ Chemical Shift Correlation Spectroscopy in Rotating Solids

B.-Q. Sun,[†,‡,⊥] C. M. Rienstra,[†,§] P. R. Costa,[†,§] J. R. Williamson,[†,§] and R. G. Griffin*[,†,§]

Contribution from the Francis Bitter Magnet Laboratory and Department of Chemistry, Massachusetts Institute of Technology, Cambridge, Massachusetts 02139-4307, and Department of Chemistry, Brandeis University, Waltham, Massachusetts 02254-9110

Received January 9, 1997. Revised Manuscript Received June 18, 1997[⊗]

Abstract: We describe 3D solid state MAS NMR experiments which separate chemical shifts in one ^{15}N and two ^{13}C dimensions. The polarization transfer from ^{1}H to ^{15}N, and subsequently to ^{13}C, is accomplished with recently developed techniques which overcome the shortcomings of constant amplitude Hartmann−Hahn cross polarization. Homonuclear ($^{13}C-^{13}C$) recoupling is performed with the MELODRAMA sequence. In the 2D $^{13}C-^{13}C$ spectra of adenosine monophosphate (AMP), successive MELODRAMA transfers propagate ^{13}C magnetization around the five ^{13}C's of the ribose ring, and the cross-peaks from successive transfer steps exhibit the negative/positive/negative... pattern expected from the double quantum polarization transfer process. The 3D $^{15}N-^{13}C-^{13}C$ spectrum of uniformly-^{15}N,^{13}C-labeled histidine consists of $^{13}C-^{13}C$ planes separated by ^{15}N chemical shifts. The 2D planes are asymmetric since in many cases the polarization giving rise to each cross-peak originates on only one nuclear spin of the coupled pair. 3D $^{15}N-^{13}C-^{13}C$ spectra of this type should be useful for dispersing overlapping spectra of peptides, proteins, and nucleic acids.

Introduction

Over the past two decades, multidimensional Fourier transform nuclear magnetic resonance (NMR) spectroscopy,[1] using various radio-frequency (RF) pulse sequences, has evolved as one of the primary methods for elucidating molecular structure.[2−4] In solution experiments, spin connectivity and molecular geometry are provided by COSY/TOCSY experiments,[5−7] and through space distances by NOESY/ROESY experiments.[8,9] The correlations in the spectra are created by polarization or coherence transfer from one spin to its neighbors, appropriately controlled by RF perturbations.

More recently, multidimensional correlation techniques have been developed for the study of the molecular structure of amorphous or polycrystalline solids.[10−12] High-resolution solid state spectra of rare spins (e.g., ^{13}C, ^{15}N, ^{31}P, etc.) subject to inhomogeneous interactions or small homogeneous interactions can be obtained by magic angle spinning (MAS) in the presence of high power heteronuclear decoupling.[13] Homonuclear dipolar couplings, which provide a measure of through-space internuclear distances, can be reintroduced into MAS spectra by imposing a "second motion" on the nuclear spin system via a train of rotor-synchronized RF pulses. Evolution of the magnetization during the mixing time of a multidimensional NMR experiment produces cross-peaks in the spectra whose intensities are proportional to the strength of the dipolar interaction.

Currently, there exists a large and expanding repertoire of pulse sequences for both homonuclear (rotational resonance (R^2),[14,15] RFDR,[16,17] DRAMA,[18] MELODRAMA,[19] DRAWS,[20] USEME,[21] RIL,[22] and C7[23]) and heteronuclear (REDOR,[24] FDR,[25,26] DCP,[27] RFDRCP,[10] and TEDOR[28]) dipolar recoupling. These methods can be distinguished by a number of

† Francis Bitter Magnet Laboratory, MIT.
‡ Brandeis University.
⊥ Present address: Schlumberger-Dull Research Laboratory, Magnetic Resonance Department, 110 Schlumberger Drive, Sugarland, TX 77478.
§ Department of Chemistry, MIT.
⊗ Abstract published in *Advance ACS Abstracts,* August 1, 1997.

(1) Ernst, R. R.; Bodenhausen, G.; Wokaun, A. *Principles of Nuclear Magnetic Resonance in One and Two Dimensions*; Clarendon Press: Oxford, 1987.
(2) Bax, A. *Annu. Rev. Biochem.* **1989**, *58*, 223−256.
(3) Wüthrich, K. *NMR of Proteins and Nucleic Acids*; John Wiley and Sons: New York, p 186.
(4) Clore, G. M.; Gronenborn, A. M. *Annu. Rev. Biophys. Biophys. Chem.* **1991**, *20*, 29−63.
(5) Aue, W. P.; Bartholdi, E.; Ernst, R. R. *J. Chem. Phys.* **1976**, *64*, 2229−2246.
(6) Bax, A.; Clore, G. M.; Driscoll, P. C.; Gronenborn, A. M.; Ikura, M.; Kay, L. E. *J. Magn. Reson.* **1990**, *87*, 620−628.
(7) Bax, A.; Clore, G. M.; Driscoll, P. C.; Gronenborn, A. M. *J. Magn. Reson.* **1990**, *88*, 425−431.
(8) Jeener, J.; Meier, B. H.; Bachmann, P.; Ernst, R. R. *J. Chem. Phys.* **1979**, *71*, 4546.
(9) Otting, G.; Wüthrich, K. *J. Am. Chem. Soc.* **1989**, *111*, 1871−1875.
(10) Sun, B.-Q.; Costa, P. R.; Griffin, R. G. *J. Magn. Reson. A* **1995**, *112*, 191−198.
(11) Griffiths, J. M.; Lakshmi, K. V.; Bennett, A. E.; Raap, J.; van der Wielen, C. M.; Lugtenburg, J.; Herzfeld, J.; Griffin, R. G. *J. Am. Chem. Soc.* **1994**.
(12) Bennett, A. E.; Griffin, R. G.; Vega, S. *NMR Basic Principles and Progress* **1994**, *33*, 1.
(13) Stejskal, E. O.; Schaefer, J. *J. Magn. Reson.* **1977**, *28*, 105−112.
(14) Raleigh, D. P.; Levitt, M. H.; Griffin, R. G. *Chem. Phys. Lett.* **1988**, *146*, 71−76.
(15) Levitt, M. H.; Raleigh, D. P.; Creuzet, F.; Griffin, R. G. *J. Chem. Phys.* **1990**, *92*, 6347.
(16) Bennett, A. E.; Ok, J.; Griffin, R. G.; Vega, S. *J. Chem. Phys.* **1992**, *96*, 8624.
(17) Sodickson, D. K.; Levitt, M. H.; Vega, S.; Griffin, R. G. *J. Chem. Phys.* **1993**, *98*, 6742.
(18) Tycko, R.; Dabbagh, G. *Chem. Phys. Lett.* **1990**, *173*, 461−465.
(19) Sun, B.-Q.; Costa, P. R.; Kosciko, D.; Lansbury, P. T., Jr.; Griffin, R. G. *J. Chem. Phys.* **1995**, *102*, 702−707.
(20) Gregory, D. M.; Mitchell, D. J.; Stringer, J. A.; Shiels, J. C.; Callahan, J.; Drobny, G. P. *Chem. Phys. Lett.* **1995**, *246*, 654−663.
(21) Fujiwara, T.; Ramamoorthy, A.; Nagayama, K.; Hioka, K.; Fujito, T. *Chem. Phys. Lett.* **1993**, *212*, 81−84.
(22) Baldus, M.; Tomaselli, M.; Meier, B. H.; Ernst, R. R. *Chem. Phys. Lett.* **1994**, *230*, 329−336.
(23) Lee, Y. K.; Kurur, N. D.; Helmle, M.; Johannessen, O. G.; Nielsen, N. C.; Levitt, M. H. *Chem. Phys. Lett.* **1995**, *242*, 304−309.
(24) Gullion, T.; Schaefer, J. *J. Magn. Reson.* **1989**, *81*, 196−200.

S0002-7863(97)00073-5 CCC: $14.00

criteria, including chemical shift offset dependence, scaling of the recoupling effect, and sensitivity to experimental imperfections. Although a complete comparison of the current methodology is beyond the scope of this work, it is important to consider the differences when selecting mixing schemes for correlation spectroscopy, particularly when two or more methods are integrated into a single experiment.

Combination of broadband homo- and heteronuclear dipolar recoupling techniques permits the observation of multidimensional chemical shift correlation spectra in uniformly isotopically labeled solid samples. As examples of these techniques, we present in this paper 2D $^{13}C-^{13}C$ spectra of uniformly-^{13}C-labeled adenosine monophosphate (AMP) and a 3D $^{15}N-^{13}C-^{13}C$ chemical shift correlation spectrum of uniformly-^{13}C,^{15}N-labeled histidine (His). The AMP spectra illustrate the ability to observe multiple connectivities using MELODRAMA. The short mixing time spectra show cross-peaks from directly bonded ^{13}C's. The longer mixing time spectra provide cross-peaks among all five ^{13}C's of the ribose ring with a pattern of negative/positive/negative... intensities for successive polarization transfer steps, as expected from the double quantum pumping operator the MELODRAMA sequence creates as the effective Hamiltonian.

The 3D $^{15}N-^{13}C-^{13}C$ spectra require the transfer of polarization from ^{15}N to ^{13}C. Although this transfer of polarization can be accomplished by a number of methods, the RFDRCP and/or adiabatic-CP sequences are demonstrated to be optimal. For $^{13}C-^{13}C$ correlation in the 3D experiment we again employ the MELODRAMA mixing sequence. The 3D spectrum of His displays $^{13}C-^{13}C$ cross peaks which are asymmetrically disposed about the diagonal, a feature which arises because the polarization is initially resident on the ^{15}N and is subsequently dispersed through the ^{13}C network. The 3D spectrum of His illustrates a strategy for assigning the ^{13}C and ^{15}N spectra of oligonucleotides, peptides, and proteins, since the signals are dispersed in multiple dimensions.

Experimental Section

2D $^{13}C-^{13}C$ and 3D $^{15}N-^{13}C-^{13}C$ chemical shift correlation experiments were performed on a custom designed spectrometer operating at Larmor frequencies of 397.8 MHz for ^1H, 100.0 MHz for ^{13}C, and 40.3 MHz for ^{15}N. The custom designed triple resonance, transmission-line MAS NMR probe[29−31] is equipped with a 4- or 5-mm spinning module assembly (Chemagnetics-Otsuka Electronics USA, Ft. Collins, CO). For the 5-mm housing, the ^1H decoupling power available was 120 kHz, corresponding to a ^1H 90° pulse length of 2.1 μs. The RF power of the ^{15}N and ^{13}C channels were set to 30−40 kHz, respectively, yielding ^{15}N and ^{13}C 90° pulse lengths of 8.5 and 6.25 μs, respectively. For the 4-mm housing, a ^1H RF field strength of 150 kHz was available. High ^1H RF field strengths during decoupling provided the appropriate mismatch from the $^{13}C/^1H$ Hartmann−Hahn condition which is required to minimize signal losses in the ^{13}C domain during recoupling experiments.[32,33] The sample spinning speed was maintained at 8 kHz and regulated to ±4 Hz by a Doty Scientific (Columbia, SC) spinning speed controller. The three samples used in the experiments were uniformly-^{15}N,^{13}C-labeled histidine; ^{15}N,α-^{13}C labeled glycine diluted to 10% to attenuate intermolecular couplings (both obtained from Cambridge Isotope Laboratories, Andover, MA); and uniformly-^{13}C-labeled AMP produced by methods described elsewhere.[34] Figure 1 shows the chemical structures and atomic numbering systems employed in assigning the 2D and 3D spectra of AMP and His.

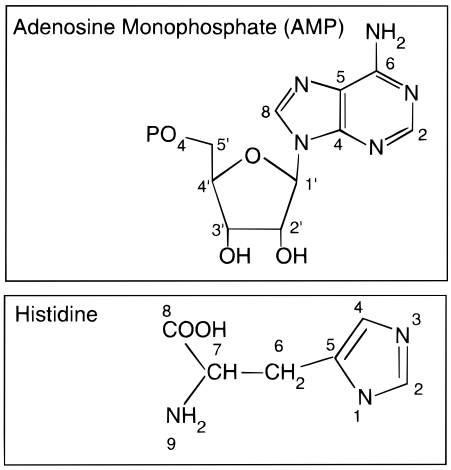

Figure 1. Chemical structures and atomic numbering systems for adenosine monophosphate (AMP) and histidine (His).

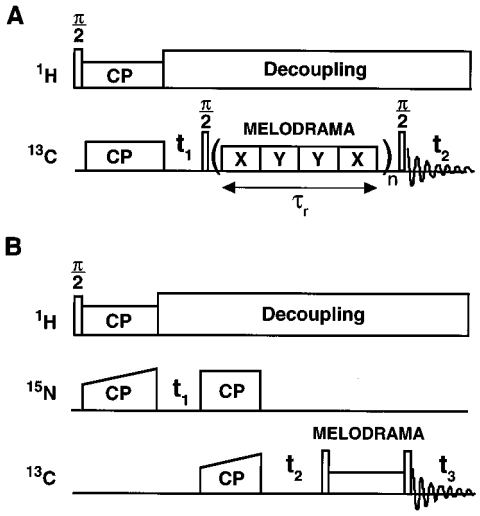

Figure 2. (A) 2D MELODRAMA sequence for homonuclear ($^{13}C-^{13}C$) dipolar recoupling. The ^{13}C rf fields are adjusted to match the condition $\omega_{rf} = N\omega_r$, typically with $N = 4$ or 5. (B) 3D NMR pulse sequence for $^{15}N-^{13}C-^{13}C$ chemical shift correlation spectroscopy. The ^1H to ^{15}N to ^{13}C transfers associated with the t_1 and t_2 periods are accomplished with RFDRCP or APHH-CP. $^{13}C-^{13}C$ recoupling is accomplished by the MELODRAMA sequence illustrated in A. Pure phase detection in all dimensions is accomplished by standard phase cycling procedures.[49,51] High power on-resonance CW decoupling is used during mixing periods, and TPPM decoupling during acquisition.[52]

The pulse sequences employed in the 2D and 3D $^{15}N-^{13}C-^{13}C$ correlation experiments are shown in Figure 2. In both sequences, cross polarization from ^1H nuclei is the initial step, directly to ^{13}C in the 2D sequence (A) and to ^{15}N in the 3D sequence (B). In the 3D sequence, the ^{15}N RF magnitude is ramped during the first CP sequence to reduce the effects of RF magnitude fluctuations (see below). After this quasi-adiabatic cross-polarization (CP) sequence, the ^{15}N magnetization evolves for a period t_1 under the isotropic ^{15}N chemical shifts. One component of the ^{15}N magnetization is then transferred to ^{13}C

(25) Bennett, A. E.; Becerra, L.; Griffin, R. G. *J. Chem. Phys.* **1994**, *100*, 812−814.
(26) Bennett, A. E.; Rienstra, C. M.; Lansbury, P. T., Jr.; Griffin, R. G. *J. Chem. Phys.* **1996**, *105*, 10289−10299.
(27) Schaefer, J.; McKay, R. A.; Stejskal, E. O. *J. Magn. Reson.* **1979**, *34*, 443−447.
(28) Hing, A. W.; Vega, S.; Schaefer, J. *J. Magn. Reson.* **1992**, *96*, 205−209.
(29) McKay, R. A. U.S. Patent No. 4,446,431.
(30) Holl, S. M.; McKay, R. A.; Gullion, T.; Schaefer, J. *J. Magn. Reson.* **1990**, *89*, 620−626.
(31) McKay, R. A. Private communication.
(32) Ishii, Y.; Ashida, J.; Terao, T. *Chem. Phys. Lett.* **1995**, *246*, 439−445.
(33) Bennett, A. E. Ph.D. Thesis, Massachusetts Institute of Technology, 1995.
(34) Batey, R. T.; Inada, M.; Kujawinski, E.; Puglisi, J. D.; Williamson, J. R. *Nucleic Acids Res.* **1992**, *20*, 4515−4523.

magnetization through application of a heteronuclear dipolar recoupling mixing sequence (RFDRCP or APHH-CP). From this point on, the 2D and 3D sequences proceed identically. The ^{13}C magnetization evolves under the isotropic ^{13}C chemical shift Hamiltonian for a period, labeled t_2 in the 3D and t_1 in the 2D sequence. During the subsequent mixing period ^{13}C magnetization exchange is driven by a broadband homonuclear dipolar recoupling sequence (e.g., RFDR, MELODRAMA, C7). During the final evolution period (t_3 for the 3D, t_2 for the 2D) the ^{13}C magnetization evolves again under the ^{13}C chemical shift Hamiltonian, while its FID is recorded.

Polarization Transfer among Low-γ Nuclei

The most common use of cross-polarization under MAS is the transfer of polarization from ^1H to low-γ nuclei. This often occurs in a regime where the heteronuclear and homonuclear couplings are large relative to the MAS rate ($|H_d^{IS}|$, $|H_d^{II}| \gg \omega_r$, where $|H_d^{IS}|$ and $|H_d^{II}|$ are the strength of the hetero- and homonuclear dipolar couplings, respectively). Large homonuclear ($^1H-^1H$) couplings broaden the Hartmann−Hahn (H−H) matching conditions,[27] so that constant amplitude matching is sufficient to drive polarization transfer, independent of small fluctuations in RF field strength, chemical shift offset, and spinning speed. However, in the limit of weak homonuclear couplings and/or rapid spinning ($|H_d| \ll \omega_r$), the width of each band in the matching profile decreases, so that satisfying the conditions $\omega_S = \omega_I \pm n\omega_r$ ($n = 1, 2$) is required.

This phenomenon is often observed in $^1H-^{13}C$ transfers at high MAS rates and/or when rapid motion averages the homonuclear and/or heteronuclear couplings (e.g., methyl groups, ferrocene, adamantane).[35] More routinely, the effects of sample spinning on the CP matching condition are observed in transfers between two low-γ nuclei. In these transfers, the absence of significant homo- and heteronuclear dipolar couplings (e.g., for ^{13}C and ^{15}N with typical dipolar couplings of 0.5−2.0 kHz) leads to the onset of sensitive matching conditions at slower spinning speeds (e.g., 2−4 kHz or faster).[27,36] At high spinning speeds and magnetic fields, the sensitivity of these matching conditions to exact RF amplitude can frustrate attempts to perform broadband $^{15}N-^{13}C$ heteronuclear chemical shift correlation experiments in rotating solids. Small differences in RF field, chemical shift, and spinning speed can cause significant changes in the matching efficiency, reducing or entirely eliminating the polarization transfer. Particularly over the extended data acquisition periods which are required in multidimensional spectroscopy, quantitative measurements require robust compensation for effective field fluctuations.

Recently several proposals have been made to circumvent sensitivities to RF magnitude and chemical shift offset. One approach is the RFDRCP sequence,[10] an improved version of SPICP,[37,38] which utilizes rotor synchronized (composite) π pulses between the simultaneous phase inversions of the SPICP sequence. Periodic inversion of the chemical shift terms in the Hamiltonian averages their effects to zero order, with the use of composite pulses in this regard minimizing the effects of RF inhomogeneity. This results in rapid (2−3 ms) polarization transfer which is stable over long periods of data acquisition.

Other methods which can be used to minimize dependence on RF magnitude rely on changing the effective field during the CP process. In the variable amplitude CP (VACP) sequence,[39,40] the amplitude of one spin-lock RF field is stepped up *and* down from a mean value, thereby sampling the appropriate range of effective fields throughout the mixing process. Ramping one field through the nominal H−H match (a unidirectional change of amplitude, from below to above the mean value) can give similar results for $^1H-^{13}C$ transfers and has the additional benefit of being quasi-adiabatic. Meier et al.[22,41] have shown that phase-shifted hyperbolic tangent ramping functions most effectively achieve the adiabatic transfer.

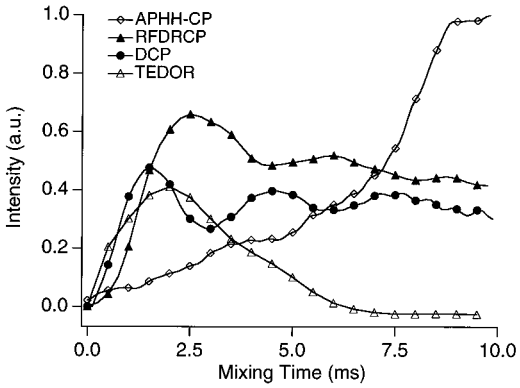

Figure 3. Transfer efficiency for four different $^{15}N-^{13}C$ cross polarization techniques. All experiments were performed at 8 kHz MAS with initial polarization created by CP transfer from ^1H to ^{15}N. On-resonance CW ^1H decoupling (120 kHz) was applied during mixing, and TPPM decoupling[52] (100 kHz, 4.8 μs switching time, ±10° phase) was used during acquisition. The intensities are normalized relative to the ^{13}C signal obtained by the optimal method, APHH-CP.

In Figure 3, we compare the cross-polarization intensity of four of these pulse sequences—constant amplitude DCP, TEDOR, RFDRCP, and APHH-CP[41]—in a $^{15}N,\alpha$-^{13}C-glycine sample. Clearly the maximum intensity is obtained with APHH-CP, which exceeds the DCP and TEDOR maxima by more than a factor of 2. In addition, we have observed that the APHH-CP is less sensitive to experimental imperfections such as RF amplitude and/or spinning speed fluctuations. However, it is important to note that the RFDRCP sequence obtains nearly 70% of the APHH-CP intensity, with a mixing time of only 3 ms. This rapid, highly efficient transfer may be of utility in cases where the size of dipolar couplings is substantially weaker than the ∼1 kHz couplings of directly bonded $^{15}N-^{13}C$ pairs. For example, two- and three-bond correlations would require substantially longer adiabatic transfer periods, which may place unreasonable demands on the probe and/or be inefficient due to competing relaxation.

MELODRAMA Spectra of AMP

After the heteronuclear chemical shift correlation is established using CP sequences, homonuclear chemical shifts can be correlated with a second mixing period. For purposes of broadband correlation spectroscopy, the method selected should (a) be independent of isotropic shift differences and CSA, (b) drive polarization transfer on a time scale which is rapid compared to incoherent signal loss (i.e., relaxation), (c) produce unambiguous correlations which have a well-understood dependence on mixing times, (d) exhibit minimal dependence on uninteresting (e.g., $^{13}C-^1H$) couplings, and (e) be generally applicable at high MAS rates.

(35) Meier, B. H. *Chem. Phys. Lett.* **1992**, *118*, 201−207.
(36) Stejskal, E. O.; Schaefer, J.; McKay, R. A. *J. Magn. Reson.* **1984**, *57*, 471.
(37) Wu, X.; Zilm, K. W. *J. Magn. Reson. A* **1993**, *104*, 154−165.
(38) Kolbert, A. C.; Gann, S. L. *Chem. Phys. Lett.* **1994**, *224*, 86.
(39) Zhang, S.; Czekaj, C. L.; Ford, W. *J. Magn. Reson. A* **1994**, *111*, 87−92.
(40) Peersen, O. B.; Wu, X.; Kustanovich, I.; Smith, S. O. *J. Magn. Reson. A* **1993**, *104*, 334.
(41) Hediger, S.; Meier, B. H.; Ernst, R. R. *J. Chem. Phys.* **1995**, *102*, 4000−4011.

In analogy to solution NMR experiments such as COSY and TOCSY,[5−7] correlation can be accomplished by polarization transfer through scalar couplings.[42] This approach has the theoretical advantage of being isotropic, which implies not only that complete transfer (for a particular value of scalar coupling) is possible but also that the analysis of orientation-dependent information measured in other dimensions is simplified. However, in order to realize these advantages experimentally, the transfer must be rapid compared to relaxation (criterion (b)). This is made difficult by the fact that in rigid solids the isotropic scalar coupling is more than an order of magnitude smaller than the dipolar coupling. Therefore the mixing times required for transfer are substantially longer (>5−10 ms for all directly bonded correlations to appear in the 2D spectrum[42]). Under typical experimental conditions, this is comparable to the rotating frame relaxation time ($T_{1\rho}$). Even at short mixing times (1−2 ms), care must be exercised to avoid substantial intensity losses.

Such intensity losses are minimized in the case of spin diffusion, a second technique for obtaining homonuclear correlations. This method relies on the indirect polarization transfer between two dipolar coupled nuclear spins through the ^{1}H reservoir.[43,44] In general, the spin diffusion rate is determined by the overlapped homogeneous lineshape and therefore depends not only on the strength of the dipolar coupling between two nuclear spins but also on their chemical shift difference. Spin diffusion has the advantage of avoiding signal losses during the longitudinal storage. However, the resulting correlation map is not always easily interpretable. In the limit of slow MAS ($|H_d| \gg \omega_r$), the magnetization exchange can be modeled by an exponential law,[33,45] but under rapid MAS the dynamics are complicated considerably, so that quantitative analysis is difficult. In some cases even qualitative information is ambiguous. For example, at high MAS rates, directly bonded unprotonated ^{13}C nuclei may have weaker correlation cross-peaks than protonated ^{13}C nuclei separated by two or three bonds. This feature has been observed in spin diffusion spectra of AMP with MAS rates of 16−18 kHz and mixing times of 5−10 ms,[46] and may limit the generality of assignment procedures for correlation spectra obtained by spin diffusion.

These ambiguities as well as the signal losses associated with scalar transfer can be avoided by using the dipolar terms in the Hamiltonian to drive polarization transfer coherently. Such an approach requires application of a dipolar recoupling sequence to interfere with MAS averaging of the relevant dipolar interactions. Although this implies some amount of signal loss during mixing due to several effects, the large size of the dipolar interaction between directly-bonded nuclei (∼2 kHz for ^{13}C−^{13}C pairs) allows for short enough mixing times (1−2 ms) that signal loss should not be significant. The coherent nature of the spin dynamics driven by the recoupled dipolar interaction furthermore implies, at least for short mixing times, a relatively straightforward relationship between cross-peak intensity and nuclear spin proximity that should allow extraction of unambiguous correlation information from the pattern and intensity of cross peaks in a typical 2D spectrum.

Several homonuclear recoupling techniques have been proposed which are sufficiently broadbanded to drive polarization transfer between spin pairs essentially independent of chemical shift in typical peptide or nucleic acid samples. These sequences include MELODRAMA, DRAWS, and C7, all of which use CW irradiation of the ^{13}C spins with a rotor-synchronized pattern of alternating RF phases to recouple the homonuclear dipolar interaction. In all three, rough matching of the rf field strength to a multiple N of the sample spinning speed is required to optimize the effect, with $N = 4$ a typical value for MELODRAMA and $N = 7$ and 8.5 for C7 and DRAWS, respectively. The relatively low RF field strength required for MELODRAMA permits application at higher spinning speeds than would be possible with the other windowless recoupling sequences under the same constraint of maximal RF fields. This is particularly important at the high spinning speeds which concentrate signal intensity in the centerband[47] and hence maximize overall S/N and spectral resolution.

Signal loss during polarization transfer periods, due to insufficient decoupling, still presents a potential problem, which is addressed by two recent proposals. The first proposal is to raise the ^{1}H decoupling field during the mixing period so that the effective decoupling field is approximately three times larger than the strength of the RF field applied on the low frequency (LF) channels.[32,33] The second proposal, described by Meier et al. (ref 42), is to implement Lee−Goldburg (LG) decoupling[48] during application of RF on LF channels. This involves setting the ^{1}H decoupling carrier frequency far off-resonance so that the effective ^{1}H RF field is aligned at the magic angle and results in a coherent averaging of the ^{1}H−^{1}H dipolar couplings in a manner analogous to MAS. The spin diffusion driven by the proton dipolar interaction is therefore minimized, and each ^{1}H−^{13}C coupled spin pair becomes more isolated than in the case of on-resonance decoupling. The dipolar recoupling sequence applied on the LF (^{13}C) channel then acts simultaneously to both recouple the ^{13}C spins and decouple the heteronuclear dipolar coupling between ^{1}H and ^{13}C nuclei. The effectiveness of heteronuclear decoupling therefore depends on the low-frequency phase modulation, and this dependence may impose an additional constraint on the design of recoupling sequences.

Such a restriction is avoided when a sufficiently large ^{1}H decoupling field is placed on resonance, as this irradiation decouples the heteronuclear interactions directly, allowing design of the LF recoupling sequence independent of the heteronuclear spin dynamics. For this reason, we find that satisfying the ∼3:1 mismatch condition of ^{1}H and LF field strengths provides optimal performance with the MELODRAMA sequence under all experimental conditions we have explored.

To demonstrate the feasibility of the MELODRAMA sequence, we present 2D chemical shift correlation spectra of uniformly-^{13}C-labeled adenosine monophosphate (AMP) with two different mixing times (Figures 4 and 5). At the short mixing time (1 ms, Figure 4), cross-peaks appear only between directly bonded nuclei. The customary connectivities can be traced from a diagonal peak to its cross-peak and then back to the next diagonal peak, etc. Thus, we see in Figure 4b that C-1′ on the sugar ring has a cross-peak with C-2′. Next, C-2′ shows a correlation with C-3′, C-3′ with C-4′, and C-4′ with C-5′. All of these cross-peaks are negative, due to the double quantum pumping operator created by the MELODRAMA sequence.

At longer mixing time (2 ms, Figure 5), the 2D MELODRAMA spectrum shows additional cross-peaks due to stepwise propagation of polarization. One- and three-step transfers are observed as negative cross-peaks; two- and four-step transfers result in positive cross-peaks. The C-1′ slice illustrates the effect, showing a negative cross-peak with C-2′, a positive peak

(42) Baldus, M.; Meier, B. H. *J. Magn. Reson.* **1996**, *121*, 65.
(43) Suter, D.; Ernst, R. R. *Phys. Rev. B* **1985**, *32*, 5608.
(44) VanderHart, D. L. *J. Magn. Reson.* **1987**, *72*, 13.
(45) Kubo, A.; McDowell, C. A. *J. Chem. Soc., Faraday Trans.* **1988**, *84*, 3713.
(46) Sun, B.-Q.; Rienstra, C. M. Unpublished results.
(47) Rienstra, C. M.; Vega, S.; Griffin, R. G. *J. Magn. Reson.* **1996**, *119*, 256.
(48) Lee, M.; Goldburg, W. I. *Phys. Rev. A* **1965**, *140*, 1261.

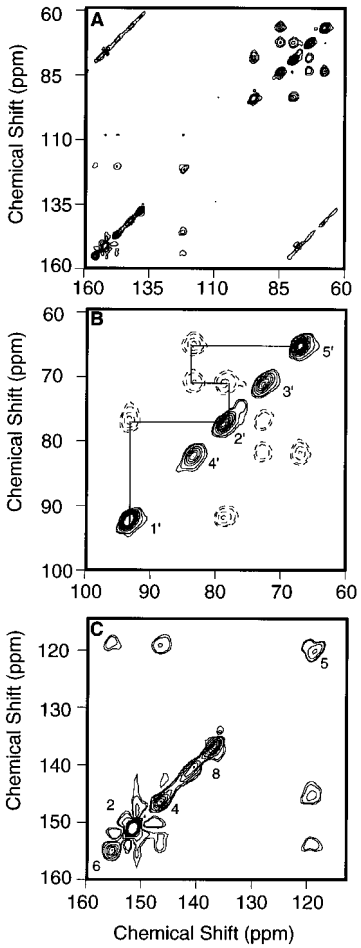

Figure 4. 2D ^{13}C spectra of U-^{13}C,^{15}N-adenosine monophosphate (AMP) with 1 ms of MELODRAMA mixing, revealing cross-peaks between directly bonded ^{13}C's: (A) entire spectrum (60−160 ppm) showing both the ribose and the adenosine regions together with sideband manifolds; (B) ribose region (50−100 ppm) displaying the strong negative absorption cross peaks between directly bonded nuclei; and (C) adenosine region (110−160 ppm) illustrating the connectivities among the aromatic ring ^{13}C signals.

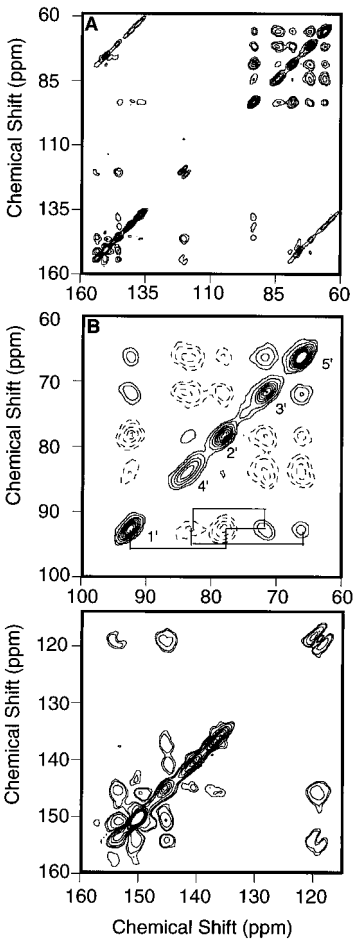

Figure 5. 2D ^{13}C spectra of adenosine monophosphate (AMP) with 2 ms of MELODRAMA mixing: (A) entire spectrum (60−160 ppm) showing both the ribose and the adenosine regions together with sideband manifolds and (B) ribose region (50−100 ppm) displaying the negative/positive/negative pattern of cross peaks among the sugar ring ^{13}C signals. The solid line cross-peaks are positive, and the dashed lines are negative. The trace at the bottom of the plot is the 1′ slice displaying the alternating cross peak pattern in one dimension: (C) adenosine region (110−160 ppm) illustrating the connectivities among the aromatic ring ^{13}C signals.

with C-3′, a second (weaker) negative peak with C-4′, and a second (weaker) positive peak with C-5′. Although the cross-peaks get progressively weaker in magnitude as the number of steps increases (a feature in common with zero-quantum polarization transfer, as in RFDR), the positive/negative feature of the double-quantum process further simplifies interpretation of multiple connectivities. In a similar manner, assignment of the adenine moiety is straightforward.

We assume in this interpretation that slower one-step transfers through two-bond (∼500 Hz) and weaker couplings do not significantly alter the appearance of the spectra. This is confirmed, at least qualitatively, by the sign of the cross-peaks observed. For example, if the rate of direct transfer from C-1′ to C-3′ exceeds the rate of two-step transfer from C-1′ to C-2′ to C-3′, the C-1′ to C-3′ cross-peak would be negative or substantially reduced in magnitude due to cancellation. This is not typically observed at mixing times on the order of 1−2 ms. Therefore, rapid successive transfers through the ∼2 kHz couplings of directly bonded ^{13}C−^{13}C are most relevant for purpose of correlation and assignment.

The Pattern of Cross-Peaks in a 3D NCC Spectrum

The cross-peaks in a typical 2D chemical shift correlation spectrum appear symmetric with respect to the diagonal, a feature which may be exploited to eliminate spurious cross-peaks through a symmetrization process. However, the 2D ^{13}C−^{13}C slices of the 3D ^{15}N−^{13}C−^{13}C spectrum of His clearly exhibit asymmetric cross-peaks. The asymmetry arises from different initial polarization of each ^{13}C site after polarization transfer from ^{15}N, consistent with the observation that the polarization is always transferred from high density to low density spin nuclei. This feature is again useful for assignment procedures, because the directionality of polarization transfer can be used as an additional constraint in confirming assignments.

In order to understand the dependence of the ^{13}C−^{13}C cross-peak intensity on the initial spin polarization, we consider a dipolar coupled homonuclear two-spin system. During the mixing time in a 2D experiment, polarization exchange is driven by the MELODRAMA sequence. The MELODRAMA zero order average Hamiltonian in the rotating frame can be written as

$$\bar{\bar{H}} = \begin{cases} D_N(I_yS_y - I_xS_x) & \text{for even } N \quad \text{(E)} \\ D_N(I_zS_z - I_xS_x) & \text{for odd } N \quad \text{(O)} \end{cases}$$

The propagator of the spin density matrix under this average Hamiltonian is therefore

$$L(t) = R_{E/O} e^{-iD_N(I_z+S_z)t} R_{E/O}^{-1}$$

where $R_{E/O}$ is the unitary operator which defines the transformation from the rotating frame into the diagonal frame of the average Hamiltonian and can be represented as

$$R_E = \frac{1}{2}E + \frac{1}{\sqrt{2}}(I_z + S_z) - \sqrt{2}(I_xS_x - I_yS_y) - 2I_zS_z$$

$$R_O = \frac{1}{2\sqrt{2}}E - \frac{1}{\sqrt{2}}(I_x + iI_y - I_z + S_x) - \sqrt{2}(I_x + iI_y - I_z)S_x$$

For simplicity we assume that the initial density matrix is

$$\rho(0) = aI_y$$

where the coefficient a is the initial polarization of I spins.

During the evolution period of the 2D experiment, spin density under the isotropic chemical shift can be expressed as

$$\rho(t_1) = a[I_y \cos \omega_I t_1 - I_x \sin \omega_I t_1]$$

At the end of the first evolution time, the MELODRAMA sequence is then applied and the spins undergo a polarization exchange process. The evolution of the spin density matrix resulting from the MELODRAMA propagator has the form of

$$\rho(t_1, \tau_m) = L_{\text{MELODRAMA}}(\tau_m)\rho(t_1)L^{-1}_{\text{MELODRAMA}}$$

$$= a\left\{\left[I_y \cos^2\left(\frac{D_N}{2}\tau_m\right) - S_y \sin^2\left(\frac{D_N}{2}\tau_m\right) - (I_x + I_z)S_x \sin(D_N\tau_m)\right]\cos \omega_I t_1 - \left[I_x \cos\left(\frac{D_N}{2}\tau_m\right) + 2I_zS_x \sin\left(\frac{D_N}{2}\tau_m\right)\right]\sin \omega_I t_1\right\}$$

We are interested in observing only the I_y and S_y components. The bilinear terms do not contribute observable coherence, but the term linear in I_x needs to be eliminated by appropriate phase cycling. This can be implemented by applying a 90° pulse alternately along the $\pm y$-axis at the end of the mixing time. Finally using the hypercomplex phase cycle,[49] we generate a set of 2D FID signals as

$$s(t_1,t_2) = a[\cos^2(D_N\tau_m/2)e^{-i\omega_I t_2} - \sin^2(D_N\tau_m/2)e^{-i\omega_S t_2}]e^{-i\omega_I t_1}$$

where ω_I and ω_S are the isotropic chemical shifts of I and S spin, respectively. The corresponding frequency domain spectrum is obtained by performing a complex 2D Fourier transformation and is represented by

$$s(\omega_1,\omega_2) = a[\cos^2(D_N\tau_m/2)\delta(\omega_2 - \omega_I) - \sin^2(D_N\tau_m/2)\delta(\omega_2 - \omega_S)]\delta(\omega_1 - \omega_I)$$

The δ-function gives two peaks in the 2D spectrum, one at $\omega_1 = \omega_2 = \omega_I$ along the diagonal and the other at $\omega_1 = \omega_I$ and $\omega_2 = \omega_S$. The intensity of the diagonal peak is $a \cos^2(D_N\tau_m/2)$, while the cross-peak intensity is $-a \sin^2(D_N\tau_m/2)$. Similarly, if the initial density matrix is bS_y, we see that the diagonal peak of the S spin has the intensity of $b \cos^2(D_N\tau_m/2)$ and the corresponding cross-peak intensity is $-b \sin^2(D_N\tau_m/2)$.

Differences in initial polarization can arise for several reasons. For example, spins may have different cross-polarization transfer efficiency, or relaxation rates during the evolution period may differ substantially. The 3D experiment represents an extreme case since the prepared ^{13}C magnetization comes predominantly from directly bonded ^{15}N nuclei. This explains why in many cases only one large cross-peak is observed in the $^{13}C-^{13}C$ 2D MELODRAMA slices.

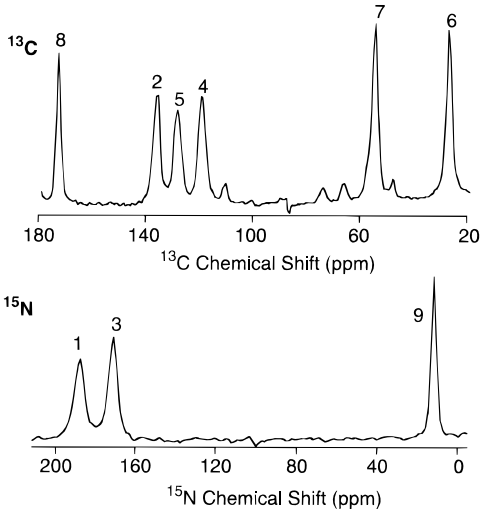

Figure 6. 1D CP/MAS spectra of U-^{13}C,^{15}N-histidine. ^{13}C and ^{15}N chemical shifts are referenced to external TMS and solid $^{15}NH_4NO_3$, respectively.

Peak Assignment of the NCC Spectrum of Histidine

Peak assignment of the 3D NCC spectrum of histidine proceeds as follows. From the ^{15}N CP/MAS spectrum (Figure 6), we see that there are only three inequivalent ^{15}N sites. The one at 0 ppm is from the amino group, and the other two at 10 and 8 ppm correspond to the N-1 and N-3 nuclei in the imidazole ring, respectively.[50] Since there are only three different ^{15}N nuclei, the three corresponding 2D slices through the ^{15}N frequency domain shown in Figure 7 include all the $^{13}C-^{13}C$ correlations. Note that the ^{15}N assignments are clearly consistent with the pattern of $^{13}C-^{13}C$ couplings in each 2D slice. In the N-9 2D slice, there is only one spectral line on the diagonal at 52 ppm, corresponding to the directly bonded C-7. We also see two negative cross-peaks from C-7 to its directly-bonded neighbors, C-6 and C-8. In the N-1 2D slice, there are two large diagonal peaks at 127 and 138 ppm corresponding to the C-5 and C-2 nuclei, respectively, assigned based on the number of negative cross-peaks each shows to directly bonded neighbors. The two negative cross-peaks to C-5 are to directly-bonded neighbors, C-4 and C-6. Combined with the information from the N-9 slice, we can assign the ^{13}C resonance at 10 ppm to C-6 and at 100 ppm to C-8. Finally, from the N-3 slice, we can assign the ^{13}C peak at 50 ppm to C-4.

Conclusions

We have demonstrated the feasibility of 3D $^{15}N-^{13}C-^{13}C$ chemical shift correlation spectroscopy in the solid state, using broadband recoupling methods which emphasize directly bonded correlations. This experiment provides unambiguous information about molecular connectivity and improved chemical shift resolution, which may assist in the assignment of peptides, proteins, and oligonucleotides. In solid state NMR, where

(49) States, D. J.; Haberkorn, R. A.; Ruben, D. J. *J. Magn. Reson.* **1982**, *48*, 286−292.

(50) Hayashi, S.; Hayamizu, K. *Bull. Chem. Soc. Jpn.* **1991**, *64*, 688−690.

(51) Marion, D.; Wuthrich, K. *Biochem. Biophys. Res. Commun.* **1983**, *113*, 967.

(52) Bennett, A. E.; Rienstra, C. M.; Auger, M.; Lakshmi, K. V.; Griffin, R. G. *J. Chem. Phys.* **1995**, *103*, 6951.

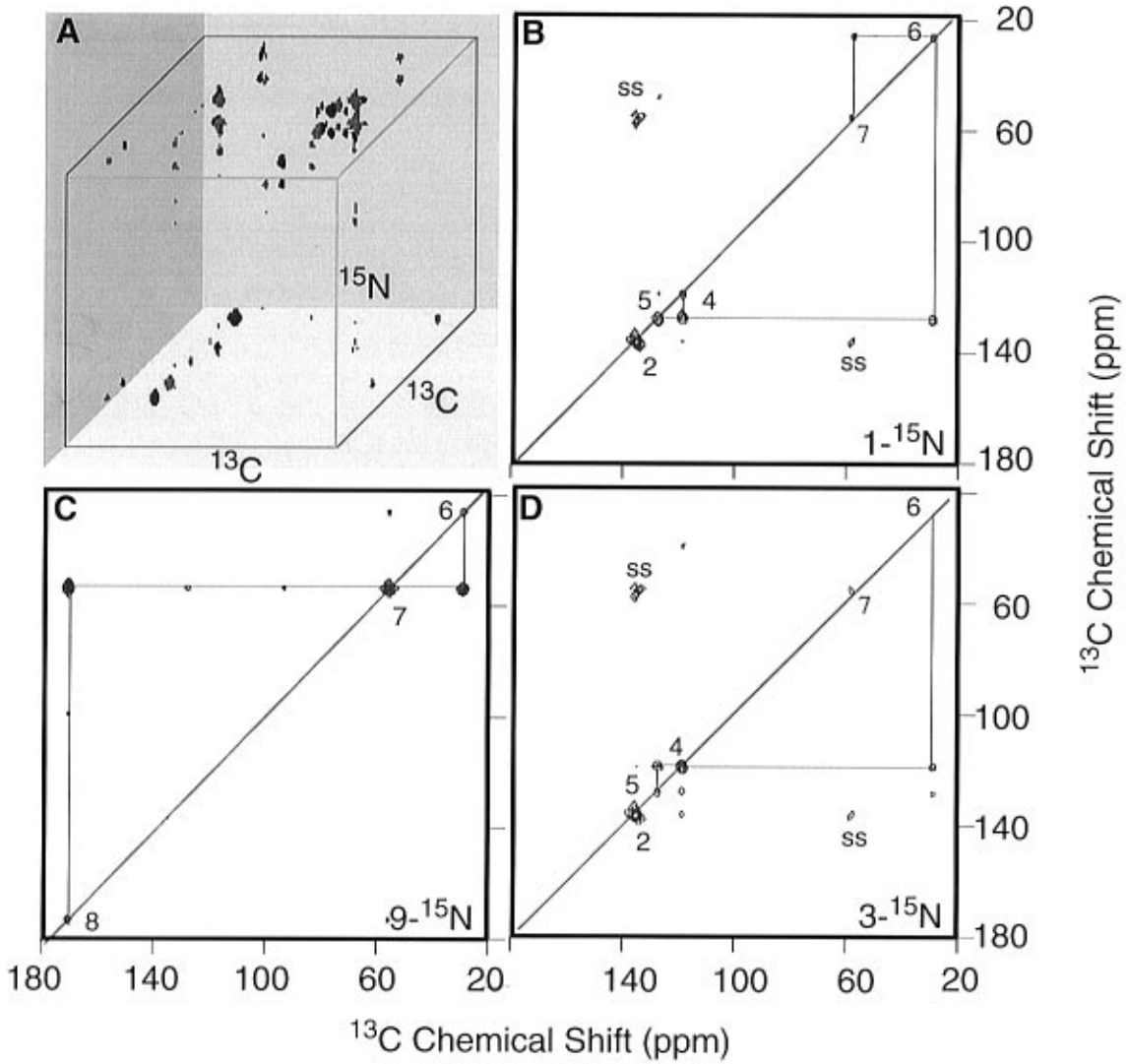

Figure 7. (A) 3D ^{15}N^{13}C^{13}C chemical shift correlation spectrum of U-^{13}C, ^{15}N-histidine showing the ^{15}N shifts on the vertical axis and horizontal ^{13}C−^{13}C planes. (B, C, D) Slices corresponding to the three different ^{15}N nuclei in the molecule (positions 1, 3, and 9). Note the ^{15}N slices show strong cross-peaks to the directly bonded ^{13}C's and weaker cross-peaks to next near neighbors generated by MELODRAMA recoupling. N-1 shows strong diagonal connectivity to C-2 and C-5, and weaker diagonal peaks corresponding to C-4 and C-6. Negative absorption cross-peaks, indicating next near neighbor bonding, are visible between C-5 and C-4, C-5 and C-6, and C-6 and C-7. A weak cross-peak between C-2 and C-4 is also visible. N-3 shows strong diagonal connectivities to C-2 and C-4 and a weaker diagonal peak corresponding to C-5. Negative and positive cross-peaks between C-4 and C-5 and between C-4 and C-6 correspond to nearest and next-nearest neighbor dipolar couplings, respectively. N-9 shows a strong diagonal connectivity to C-7 and weaker diagonal peaks corresponding to C-6 and C-8.

resolution and sensitivity are the primary limitations to a vast number of new applications, methods for chemical shift correlation which minimize signal loss are crucial. With future improvements in decoupling methodology, we anticipate extension of this approach to 4D correlation experiments involving, for example, ^{31}P in oligonucleotides. In addition, the mixing sequences can be altered for the measurement of additional parameters in a similar fashion. For example, the chemical shift anisotropy may be reintroduced by appropriate mixing schemes and correlated to isotropic shifts in one or more additional dimensions, thereby providing a measure of relative tensor orientations for many molecular connectivities in a single experiment. These and related methods should greatly increase the number of systems which are amenable to structural study by NMR in the solid state.

Acknowledgment. The authors wish to acknowledge support of this research by NIH Grants GM-36810, GM-23403, GM-23289, and RR-00995. We thank Prof. Judith Herzfeld (Brandeis University), John D. Gross, and Dr. Mary E. Hatcher for assistance in reading and revising drafts of the manuscript. Chad M. Rienstra is a Howard Hughes Medical Institute Predoctoral Fellow.

JA970073R